Journal of the European Ceramic Society **16** (1996) 239–247

0955-2219(95)00157-3
0955-2219/96/$15.00

Phase Transformation and Grain Coarsening of Zirconia/Mullite Composites

Wen-Cheng J. Wei, H. C. Kao & M. H. Lo

Institute of Materials Science and Engineering, National Taiwan University, Taipei, Taiwan 106, Republic of China

(Accepted 22 July 1995)

Abstract

ZrO_2/mullite composites (ZMC) with homogeneously dispersed ZrO_2 grains were prepared from colloidal or sol–gel processes of the precursors, which were a mixture of colloidal pseudo-boehmite (γ-AlOOH), zirconia and silicic acid gel, or prepared from dissociated zircon with alumina powder. After pressureless sintering of the ZMCs, their microstructure was examined by means of X-ray diffractometry, scanning electron microscopy and analytical transmission electron microscopy techniques. The microstructure of the ZMCs showed a difference in scale. ZrO_2 and mullite grains grown in the gel matrix were formed at temperatures as low as 1100 and 1300°C, respectively. Experimental results indicated that heat treatment from 1300 to 1600°C influences the growth of mullite and fine ZrO_2 grains in ZMCs, especially for the composite prepared from sol–gel methods in which the ZrO_2 grew from tens of nanometres to micrometre size. The effects of the presence of ultra-fine ZrO_2 on retarding the grain growth of mullite and the increase of metastable t-phase ZrO_2 are also discussed. The growth of fine ZrO_2 grains in a mullite matrix belongs to a mechanism of coalescence.

1 Introduction

The appropriate selection of a matrix phase and the addition of various zirconia grains to form ceramic composites with better strength and toughness has become widely recognised as a method for producing materials for engineering applications. ZrO_2 in alumina,[1] Si_3N_4[2] and mullite[3] have been reported to form composite systems that are effective in strengthening and toughening the ceramic matrix. Garvie[4] also found that the addition of 10% tetragonal (*t*) zirconia enhanced the thermal shock resistance of zircon–zirconia composite. The retained strength of zirconia–zircon composites could be as high as 90% of the original after quenching from 600°C. In addition, other advantages included less deterioration as a result of the tetragonal to monoclinic (*m*) phase transformation of zirconia grains at high temperature and in high humidity environment, and more economically feasible materials owing to lower costs. However, some disadvantages were also recognised: the zirconia particles coarsened in the alumina matrix[5] as soon as the ceramic matrix densified. Also, thermal expansion mismatch of ZrO_2 with the ceramic matrix resulted in thermal stresses, either tensile or compressive, as the zirconia composite was cooled from sintering temperature. These would trigger the '*t*-to-*m*' transformation, thereby degrading mechanical properties.

High quality mullite can be made from various sources, alkoxides or other high purity chemicals, through the sol–gel or co-precipitation method.[6] The method allows the addition of zirconia for making zirconia-toughened mullite (called ZMC in this paper) composites. In addition, the composites can also be made by the reaction sintering of zircon and alumina,[7,8] by the co-sintering of fine zirconia/mullite mixture,[9] or by directly sintering the mixture of alumina, silica and zirconia.

High temperature densification above 1450°C with sintering aids is currently used to densify the zirconia–mullite composite. TiO_2,[3] MgO[10,11] and Ca[12] can facilitate the formation of a liquid phase to achieve viscous sintering. These additives were reported to have a profound influence on the high temperature properties of ZMC[8] and on the formation of glassy and grain boundary phases.[10]

The additives, including ZrO_2 and sintering aids, may dissolve in the mullite matrix to some extent. A microanalysis experiment to determine the ZrO_2 content in mullite grains was conducted by Dinger *et al.*,[13] who found the presence of an apparent solid solution on the crust of mullite grains. This gave a grain boundary of mullite in a state of expansion, thereby improving the toughness of the composite. Other oxide dopants, including Ti, V, Mn, Fe and Co oxides,[14] incorporated into

the mullite structure were determined as being preferentially located in oxygen octahedral sites. The upper limit of solubility is controlled by cation radii and the valence state of cations. This work was partially motivated by the report that the amount of ZrO_2 solid solution in mullite composites was of the order of few per cent up to 20%,[13] which was thought to be quite influential in determining the grain growth mechanism of ZrO_2.

Since the toughness and high temperature stability of ZMC are dependent upon the reactions between zirconia and mullite phases, gel-derived precursors and high purity zircon reacted with alumina are used here with and without sintering additives. This research attempts to characterize the transformation of ZrO_2 and the microstructural features, as well as determine the coarsening phenomenon of zirconia and mullite. Thus, rationalizing the parameters which govern the grain growth phenomenon is of interest, thereby permitting the development of an appropriate quantitative model.

2 Experimental

2.1 Sample preparation

2.1.1 Gel-derived (GD-) ZMC

The solution prepared for gelation included 50 wt% tetraethyl orthosilicate (TEOS; Merck Chemical Co., Germany), 30 wt% dry alcohol (reagent grade; Showa Chemicals Co., Ltd, Tokyo, Japan) and 20 wt% 0·018 N HCl (diluted from regent grade 0·1 N HCl; Merck Chemical Co., Germany). The three chemicals were first mixed and then maintained in a water bath at 50°C for 3 h, so as to obtain a well-mixed silicic acid solution.[6] Next, pseudo-boehmite sol (Remet Co., NY, USA) and ZrO_2 sol (Johnson Matthey Co., MA, USA) were slowly added to the solution. After mixing for 30 min, the viscosity of the solution increased until gelation. The gel was dried at 80°C for several days until no further weight loss was measured. The aerogel was crushed and sieved through 325 mesh. The Al_2O_3 and SiO_2 ratio was at the mullite stoichiometry and the volume fraction of added ZrO_2 was 24, 9 or 3 vol%. ZMC powders were die-pressed at a pressure of 160 MPa. Sintering of the specimens was conducted at 800 to 1600°C for 2 to 6 h.

2.1.2 Reaction-sintered (RS-) ZMC

Two types of RS-ZMC mixture were selected as comparative cases.[15] One was a mixture of dissociated zircon (supplied by Z-Tech Corp.; impurities included 0·36% Al_2O_3, 0·08% TiO_2, 0·03% Fe_2O_3, and 0·11% free SiO_2) and alumina (A-16SG; Alcoa Corp., USA) powders. The other consisted of ground zircon sand, alumina and 4 wt% CeO_2 as a sintering aid. They are named DZ-ZMC and RS(CeO_2)-ZMC, respectively. The zircon/alumina mixtures were in a molar ratio of 2:3, subsequently yielding 24 vol% ZrO_2. These powders were initially dispersed in distilled water with 1 wt% dispersant (based on solid phase; Darvan C, supplied by R.T. Vanderbilt Co., USA), then turbo-mixed for 2 h. The solid fraction of the slurry was 30 vol%. After being cast and dried on a plaster mould, the CeO_2-doped RS-ZMC was sintered between 1400 to 1550°C for 2 h; however, the DZ-ZMC was sintered at higher temperatures, from 1400 to 1700°C (which is higher than the dissociation temperature of zircon) for 30 min. The heating rate of the sintering was 10°C min^{-1}. Nearly fully-dense DZ-ZMC and RS-ZMC samples were obtained, then heat-treated at temperatures from 1400 to 1700°C.

2.2 Characterization

Densification of the ZMCs was examined by a dilatometer (Theta Industries, Inc., USA) up to 1500°C. Crystalline phases were determined by X-ray diffractometry (XRD; PW 1729, Philips Electronics Instruments, Inc., USA). Microstructural and micro-chemical analyses were performed by using scanning electron microscopy (SEM; Philips 515) and transmission electron microscopy (TEM; JEOL 100CXII and 2000FX, JEOL Inc., Japan), the latter equipped with EDAX (Tracer Northan Co., USA). The densities of the sintered specimens were obtained by Archimedes' method.

3 Results and Discussion

3.1 Transformation sequence

The XRD patterns of three ZMC powders were analysed and are summarized in Table 1. GD-ZMC appeared to have no crystalline phases when sintered at 800°C for 2 h. Tetragonal-ZrO_2 and mullite phases appeared at 1100 and 1300°C, respectively. The peak width of the *t*-phase ZrO_2 at 1100°C in Fig. 1 is apparently broader than the diffraction peaks of *t*-ZrO_2 at temperatures ≥1200°C. This implies that the zirconia has a fine grain size. After sintering at temperatures of 1600°C or above, a large portion of ZrO_2 transforms to *m*-phase in the GD-ZMC. As for the RB-ZMC, only about one-third of the ZrO_2 was found to be the tetragonal phase at sintering temperatures above 1450°C, but this quantity decreased with increasing sintering temperature and CeO_2 additive, as shown in Fig. 2. This decrease could be due to grain growth of the

Table 1. Phases detected in ZMCs prepared from three different sources and sintered at temperature shown for 2 h

GD-ZMC							
phase/temp.	1000	1100	1200	1300	1400	1500	1600 (°C)
Zircon	—	—	*	*	*	—	—
Mullite	—	—	—	*	*	*	*
t-ZrO_2	**	**	**	**	**	*	*
m-ZrO_2	—	—	—	—	—	*	**
RS-ZMC (without additive)							
phase/temp.	1400	1450	1500	1550 (°C)			
Zircon	**	**	*	*			
Mullite	—	—	*	*			
t-ZrO_2	—	—	*	*			
m-ZrO_2	—	—	*	**			
RS-ZMC (with 4 wt% CeO_2 additive)							
phase/temp.	1400	1450	1500	1550 (°C)			
Zircon	**	*	*	*			
Mullite	—	*	*	*			
t-ZrO_2	—	—	*	—			
m-ZrO_2	—	*	*	**			

Note –, * and ** means that the X-ray diffraction intensity of the phase is not detectable, detectable and in large quantity, respectively.

ZrO_2, lack of phase stabilizer such as CaO or MgO, and thermal stress induced transformation. However, the amount of t-ZrO_2 finally became stable at a level of 20% (Fig. 2) when the heat treatment was extended up to 4 h at 1450°C. This occurrence is explained later by means of microstructural observations (in Section 3.3), in which the t-ZrO_2 is possibly intragranular and holds a submicrometre size.

The formation temperatures of these zirconia and mullite phases in GD-ZMC are apparently lower than the RS-ZMCs, as shown in Table 1, and are also lower than those reported by Low and McPersonal.[16] GD-ZMC underwent this transformation at a temperature 200°C lower than that for RS-ZMC.[17] This lower transformation is due to the reaction kinetics, enhanced by the fact of the diminutive gel structure in GD-ZMC.

Zircon, as a reaction product of zirconia and silica, forms as a transition phase in the gel-derived ZMC in the range between 1200 and 1500°C. If the temperature increases, the amount of zircon phase decreases and is accompanied by the appearance of mullite phase. The formation and diminishing of zircon phase in a similar ZMC

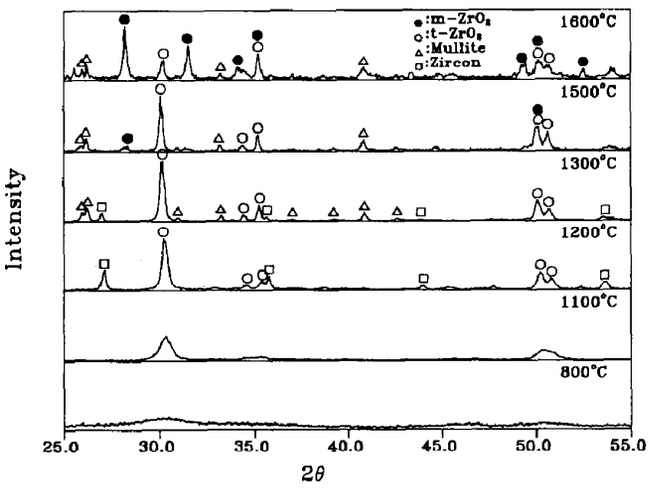

Fig. 1. XRD patterns for GD-ZMC samples after sintering at 800 to 1600°C for 2 h.

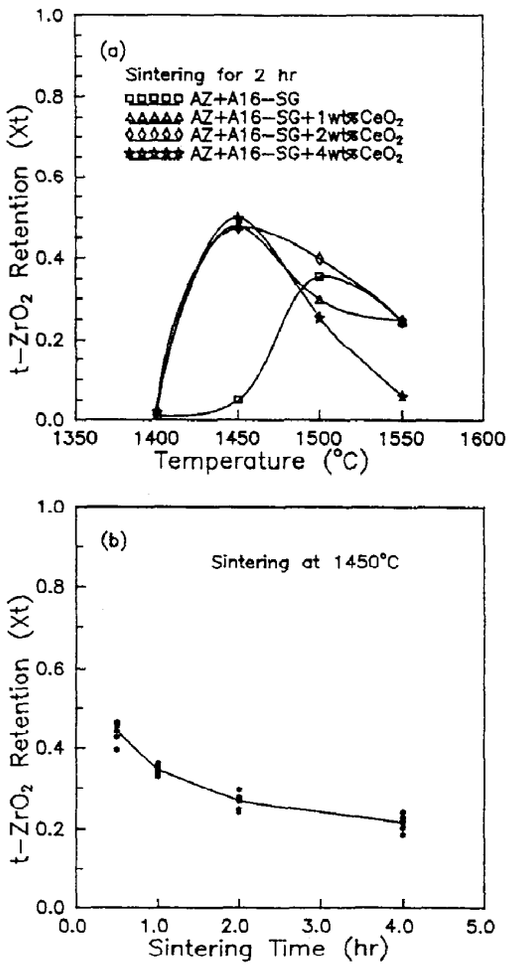

Fig. 2. Weight fraction of t-phase zirconia in reaction-sintered RS-(CeO_2)-ZMC as a function of (a) sintering temperature and (b) sintering time at 1450°C.

was also reported by Holmstron *et al.*,[18] who used Al_2O_3, SiO_2 and ZrO_2 as raw materials to prepare a reaction-sintered ZMC. The zircon appeared at temperatures between 1450–1560°C when the ZrO_2 content was >15 vol%. In this study, the spray-dried powders were found to have phase transformation sequences similar to those of the powders prepared from grinding.

3.2 Densification of ZMCs

Dilatometric data of the ZMCs are shown in Fig. 3 plotted as a function of sintering temperature up to 1500°C. The changes in the dimensions of die-pressed GD-ZMC at temperatures around 300 and 550°C correspond to the sintering of extremely fine pores, in which the contained volatile species evaporate readily. Those nm size pores are densified at 600°C or lower temperatures, as reported previously.[6] Testing at higher temperature unveils that the next densification of GD-ZMC starts at 900°C and exhibits the fastest densification rate at 1200°C. In comparison, DZ- or RS-ZMC specimens undergo less densification and at higher temperature starting from 1100°C. The densification rate of RS-ZMC can be enhanced by the addition of CeO_2, as revealed by the densification curve of the RS(CeO_2)-ZMC in Fig. 3. The GD-ZMC shows a lower sintering temperature and more shrinkage than the other two ZMCs.

3.3 Microstructural evolution

Figure 4 shows SEM micrographs of polished and thermally-etched RS- and DZ-ZMC samples. The micrographs show dense and well reacted ZMCs, which have a relative density of >95% TD (theoretical density). The densified ZMCs show very stable microstructural features, most of the intergranular ZrO_2 being 3 μm in size (Fig. 5), as they are post-annealed at temperatures of 1400 to 1600°C for up to 24 h. The grain sizes of mullite and ZrO_2 change within the range of experimental error, so that their grains are considered not to coarsen during the heat treatment. Some fine and submicrometre-sized zirconia grains are observed

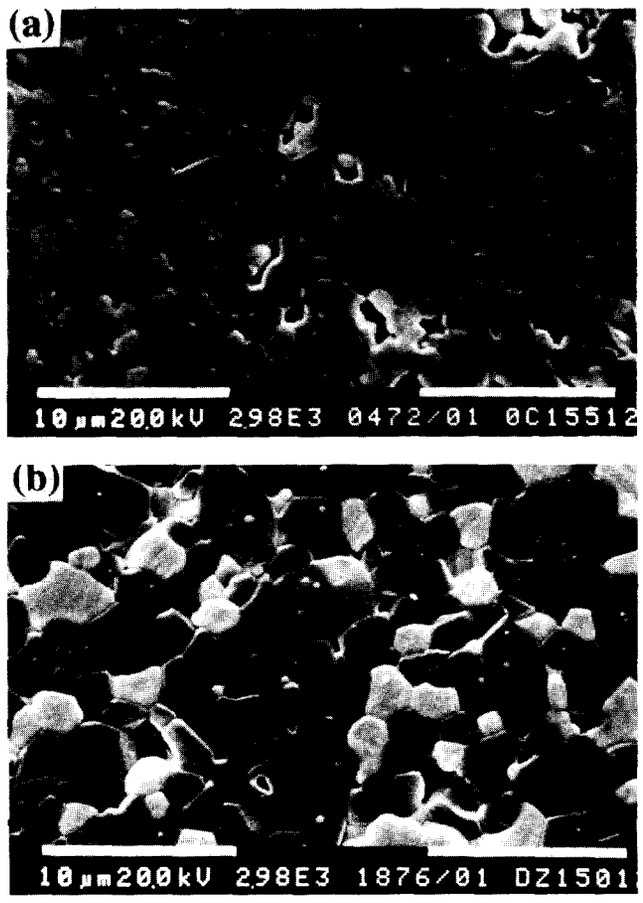

Fig. 4. SEM micrographs of (a) RS-ZMC without doping additive sintered at 1550°C for 12 h; (b) DZ-ZMC sintered at 1700°C for 30 min, then annealed at 1500°C for 12 h. The samples were all polished and thermally etched.

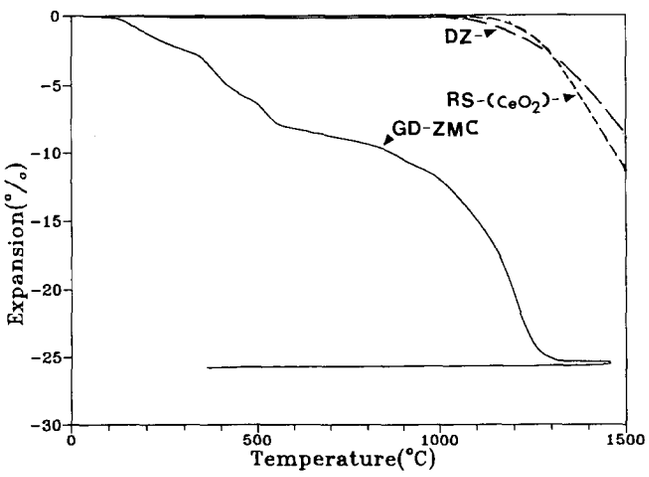

Fig. 3. Dilatometric curves of gel-derived (GD), reaction-sintering with 4 wt% CeO_2 (RS-(CeO_2)-) and DZ-ZMC specimens plotted as a function of temperature.

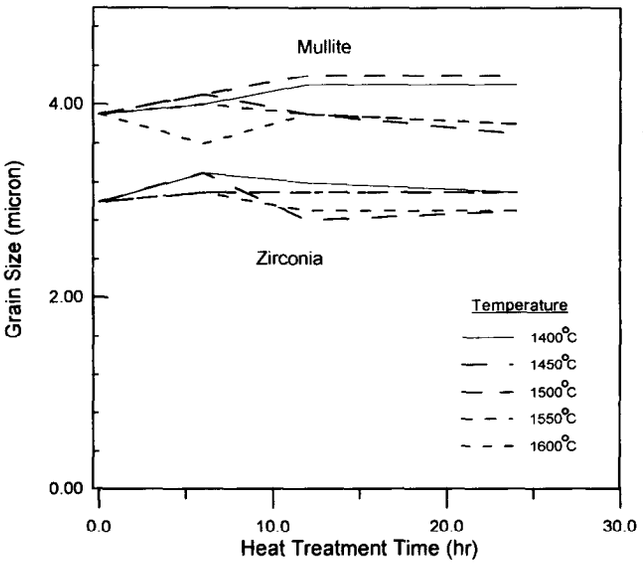

Fig. 5. Average grain sizes (μm) of intergranular zirconia and mullite grains of DZ-ZMC samples with 24 vol% ZrO_2 sintered at 1700°C for 30 min following various heat treatments.

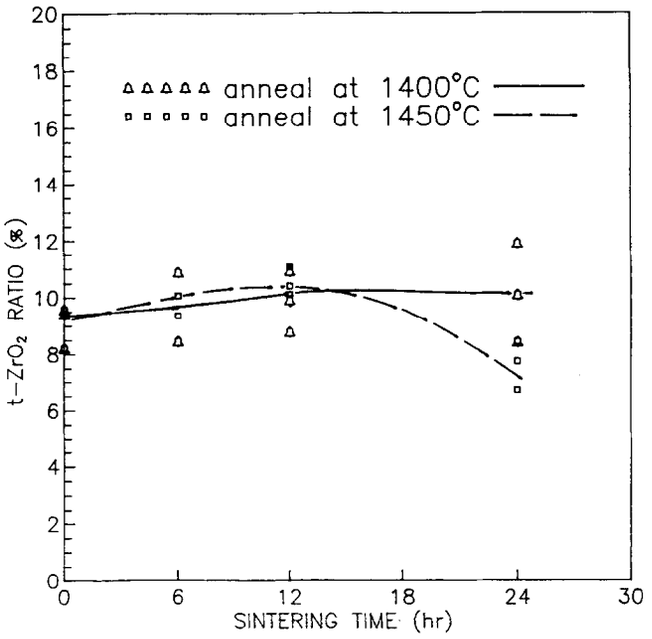

Fig. 6. Weight percentage of t-ZrO_2 phase to all ZrO_2 in DZ-ZMC vs. annealing period at 1400 or 1450°C.

that are nearly spherical and engulfed in mullite grains (Fig. 4). These intragranular ZrO_2 grains are the major part of t-phase ZrO_2 which is not transformable even following the same post-annealing at 1400 or 1450°C as long as 24 h (Fig. 6). The microstructures of the RB-ZMCs are stable at high temperatures (> 1400°C). However, the reaction-sintering process for the preparation of ZMC cannot offer the microstructure with finer ZrO_2 and submicrometre-sized mullite grains.

GD-ZMC samples sintered at 1400, 1500 or 1600°C for 2 h were carefully polished and thermally-etched at the conditions 1350°C for 2 h, 1475°C or 1500°C for 30 min, respectively. The GD-ZMC sample sintered at 1600°C [Fig. 7(c)] has a similar microstructure to the previous RS-ZMCs. A small fraction of fine-grained zirconia is enclosed in the mullite grains, which are of the order of a few micrometres in size. Figures 7(b) and (c) clearly show that ZrO_2 grains are either intergranular or intragranular; the grain size of intergranular ZrO_2 increasing with sintering temperature. The intragranular ZrO_2 in the 1400°C and 2 h sintered sample is $< 0{\cdot}1$ μm. If sintered at 1600°C for 2 h, it grows to 2·3 μm and becomes intergranular. Increasing the size of ZrO_2 grains has been shown previously to instantly transform ZrO_2 to m-phase.[5] The analysis of XRD patterns in Fig. 1 reveals several strong diffraction peaks of the m-phase in the pattern of the 1600°C sintered samples; however, the m-phase is rarely detected in the GD-ZMC processed at 1500°C or lower temperatures.

It is noted that the amount of intragranular ZrO_2 decreases with increasing sintering temperature. Meanwhile, the average grain sizes of the intergranular ZrO_2 and matrix mullite grow larger. The grain size data, obtained from SEM and TEM micrographs, reveal that the intergranular ZrO_2 and matrix mullite grains scarcely grow from 1300 to 1500°C. However, both phases grow rapidly in size when the sintering temperature rises from 1500 to 1600°C.

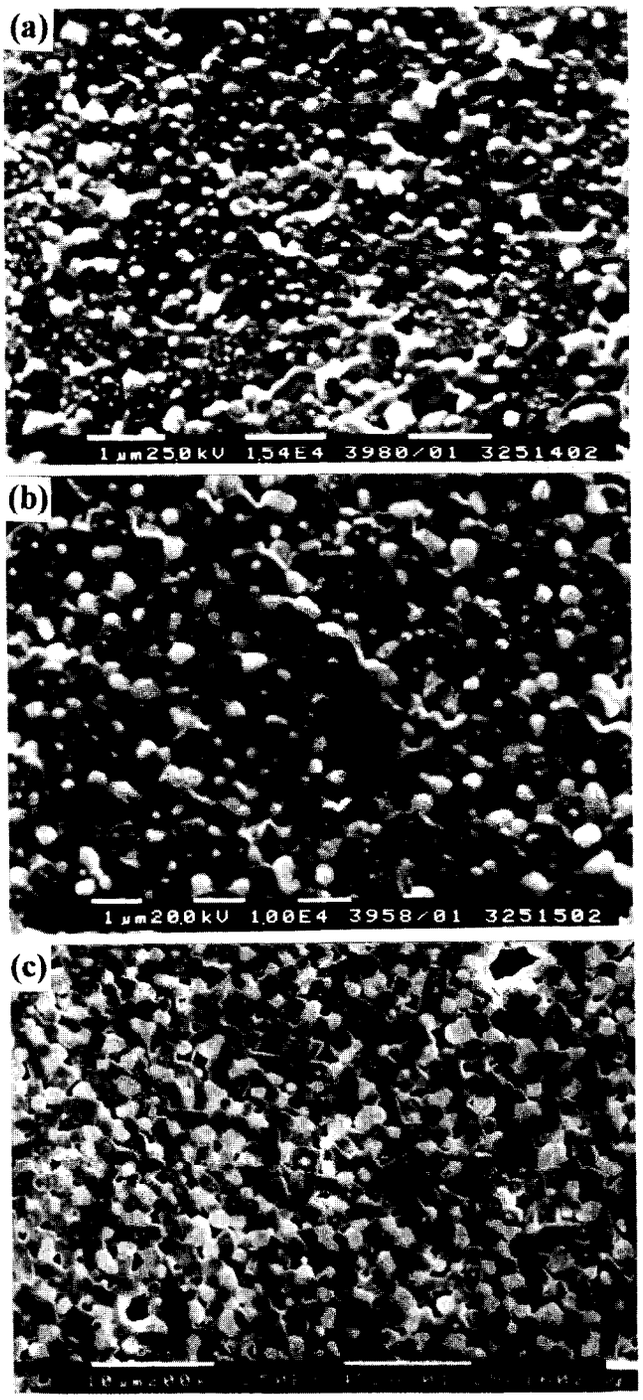

Fig. 7. SEM micrographs of polished and thermally etched GD-ZMC specimens sintered at (a) 1400°C, (b) 1500°C and (c) 1600°C for 2 h.

TEM bright-field (BF) and centred-dark-field (CDF) micrographs of a GD-ZMC sample sintered at 1300°C for 2 h are shown in Fig. 8. The BF image shows that the ZrO_2 grains in dark

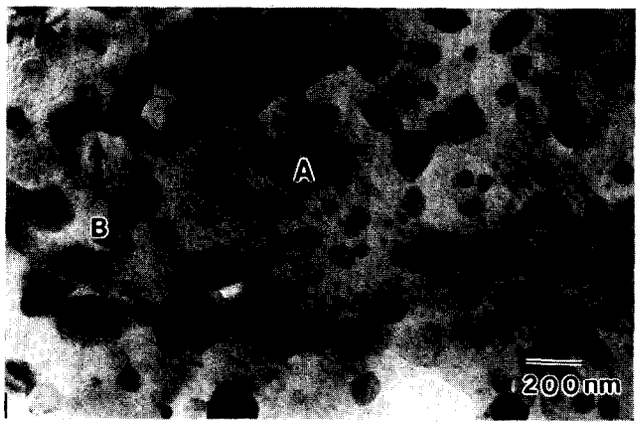

Fig. 8. TEM BF micrograph of GD-ZMC (with 24 vol% ZrO_2) sintered at 1300°C for 2 h.

contrast are uniformly dispersed within the mullite matrix. For sintering at higher temperature, a few large (0·3 μm or larger) intergranular ZrO_2 grains are occasionally found in the 1400°C sintered GD-ZMC. The twinning features of these grains (Fig. 9) are characteristic of *m*-phase ZrO_2. The boundaries of each ZrO_2 lath in the large *m*-ZrO_2 grains exhibit interfacial microcracks, as denoted by arrows A and B in Fig. 9. In addition to the microcracks, strain fringes (arrow C) occurring next to large ZrO_2 grains are produced by thermal mismatch, and represent internal stresses.[19] These features, i.e. microcracks and strain fringes, are possibly caused by the phase transformation of *t*-ZrO_2 to *m*-ZrO_2 and thermal expansion mismatch between mullite and ZrO_2.

SEM and TEM analyses indicate that GD-ZMC has a smaller grain size than DZ- or RS-ZMC when sintering at the same temperature. For 24 vol% ZrO_2 samples, the average grain size of the intergranular ZrO_2 in GD-ZMC is 98 nm and the size of the mullite grains is 600 nm, which is

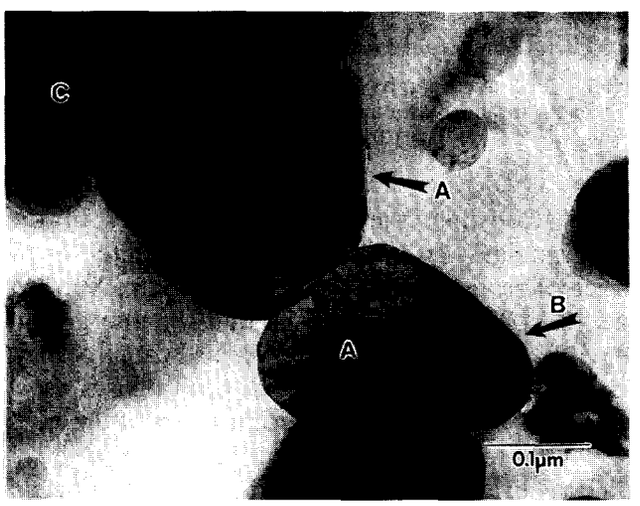

Fig. 9. Microcracks (A and B) and strain fringes (C) around two overgrowth *m*-ZrO_2 grains, imaged with TEM BF conditions. The GD-ZMC was sintered at 1400°C for 2 h.

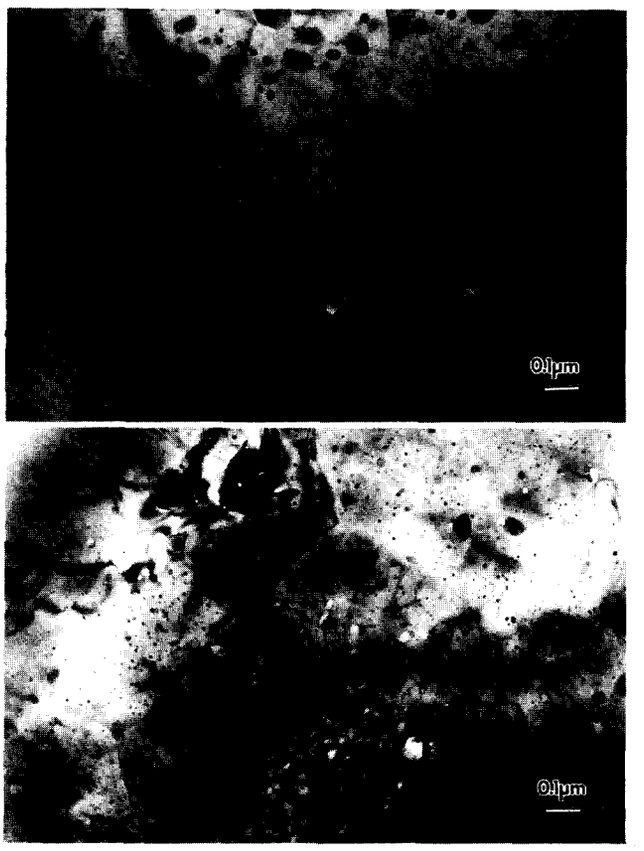

Fig. 10. TEM micrographs of GD-ZMC samples with (a) 9 vol% and (b) 3 vol% of ZrO_2 sintered at 1400°C for 2 h.

several times less than the size of mullite grains measured in a pure aluminosilicate gel system.[6] However, the mullite grows to a larger size if sintered at a higher temperature or the composition contains less ZrO_2. Figure 10 presents TEM micrographs of GD-ZMC samples containing either 9 or 3 vol% ZrO_2. Their ZrO_2 grains are mostly intragranular, and have an average grain size, 30 or 9 nm, which is several times less than that of GD-ZMC with 24 vol% ZrO_2. The mullite grains in Fig. 10 grew to larger size, near 1 μm, and had straight grain boundaries. The dragging of mullite grain boundaries by ZrO_2 grains is apparently dependent upon the volume fraction and size of the ZrO_2, which is similar to the behaviour reported by Lange and Hirlinger[20] and Prochazka *et al.*[9] An illustrative example, i.e. the 1300°C-sintered GD-ZMC sample, is given in Fig. 8; the mullite grains exhibit crooked boundaries which trap several larger ZrO_2 grains (larger than the average size of intragranular ZrO_2). This demonstrates the likelihood that the growth of mullite grains is inhibited by ZrO_2 grains.

3.4 Grain growth of zirconia and mullite

The results of previous SEM and TEM micrographs are reported in Fig. 11, from which it can be seen that the grain sizes of mullite and ZrO_2 in

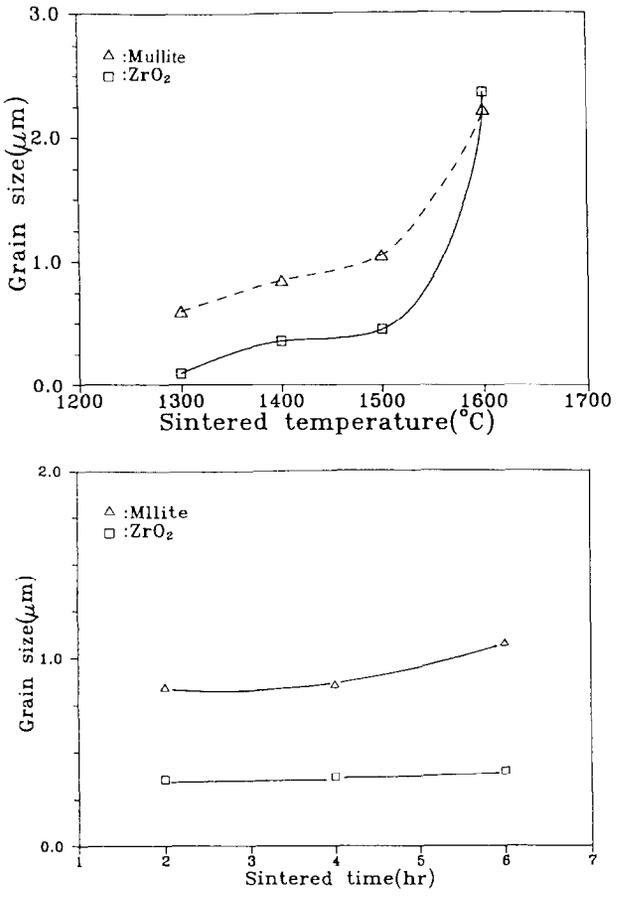

Fig. 11. Grain sizes of mullite and intergranular ZrO_2 in various GD-ZMC samples with 24 vol% ZrO_2: (a) sintered at 1300 to 1600°C for 2 h; (b) sintered at 1400°C for 2 to 6 h.

various gel-derived ZMCs increase as the sintering temperature and sintering time increase. The application of Zener's relationship[21] to the above cases illustrates the relationship between the mean grain radius (R) of the mullite matrix, the mean radius (r) of the ZrO_2 inclusions and the volume fraction (f) of the inclusion:

$$R = 4\,r/(3\,f) \tag{1}$$

This relationship provides a calculated R value for the 1400°C-sintered GD-ZMC that is comparable with the measured R (Table 2). However, the measured mullite grain size increases as the amount of zirconia decreases, and the zirconia inclusions are not all spherical and uniformly distributed (Fig. 10), leading to differences between measured and calculated R values. In addition, the relationship does not hold true for mullite grains in the GD-ZMC sintered at temperatures >1500°C [Fig. 11(a)]. The growth of the mullite grains is accompanied by the coarsening of ZrO_2 inclusions. Two phases are growing inter-affected.

Table 2. Calculated and measured mean radius (R) of mullite in GD-ZMC determined from the volume fraction (f) and grain radius (r) of zirconia phase

f	r (*nm*)	*Calculated* R (*nm*)	*Measured* R (*nm*)
0·24	49	272	300
0·09	15	222	~600
0·03	4·5	200	~750
Pure mullite[22]	—	—	~1250

The second-phase ZrO_2 in the mullite matrix can ripen either by Ostwald ripening or by coalescence. The processes are well documented in a similar ceramic composite system,[5] in which Ostwald ripening is driven by the variation of solubility of ZrO_2 with various particle sizes, and the composite grows larger ZrO_2 particles at the expense of smaller ZrO_2 particles. Coalescence of ZrO_2 particles occurs by the dragging of matrix mullite boundaries. The phenomenological evidence for the former process was a particle-free zone at matrix grain boundaries despite the fact that the diffusion rate along the mullite grain boundaries is faster than that in the mullite lattice. Alternatively, the latter case is particle clustering at grain boundaries. In this study, the micrographs revealed no grain boundary particle-free zone.

It was reported by Dinger *et al.*[13] that a 2% solid solution of ZrO_2 near interface grain boundaries of mullite has been detected. They sintered the sample at 1570°C for 2 to 16 h. Mullite with an extensive amount of zirconia solid solution should be expected at temperature >1570°C. But a quite controversial result was reported later by the same research group,[10] that >20 wt% of ZrO_2 was found in the mullite grains. This seems *not to be the case* for our ZMC. Figure 12 shows a DZ-ZMC sample that has been sintered at 1700°C for 30 min. The zirconia grains either intergranularly or intragranularly are of size 50 nm to 3·5 μm, as shown in Fig. 12. Scanning transmission electron microscopy with micro-beam EDS analysis reveals that the ZMC has a non-detectable zirconia concentration in the mullite grains, as shown in the EDS spectra obtained from spots 2 and 4. That implies that *no zirconium forms a solid solution in mullite.* This finding is consistent with the recent measurement given by Moya[23] that <0·1 wt% zirconia solid solution is measured in zirconia-toughened mullite. This implies that ripening through grain boundary diffusion was not occurring in ZMC. Many intergranular ZrO_2 particles are actually in the form of clustering at triple grain boundaries, and exhibit larger grain size. We believe that such particle clustering is good evidence for coarsening by the coalescence of ZrO_2. The zirconia in GD-ZMC is apparently ripening intergranularly while being treated above 1300°C in this experiment.

4 Summary

Three types of ZMC prepared either from gel

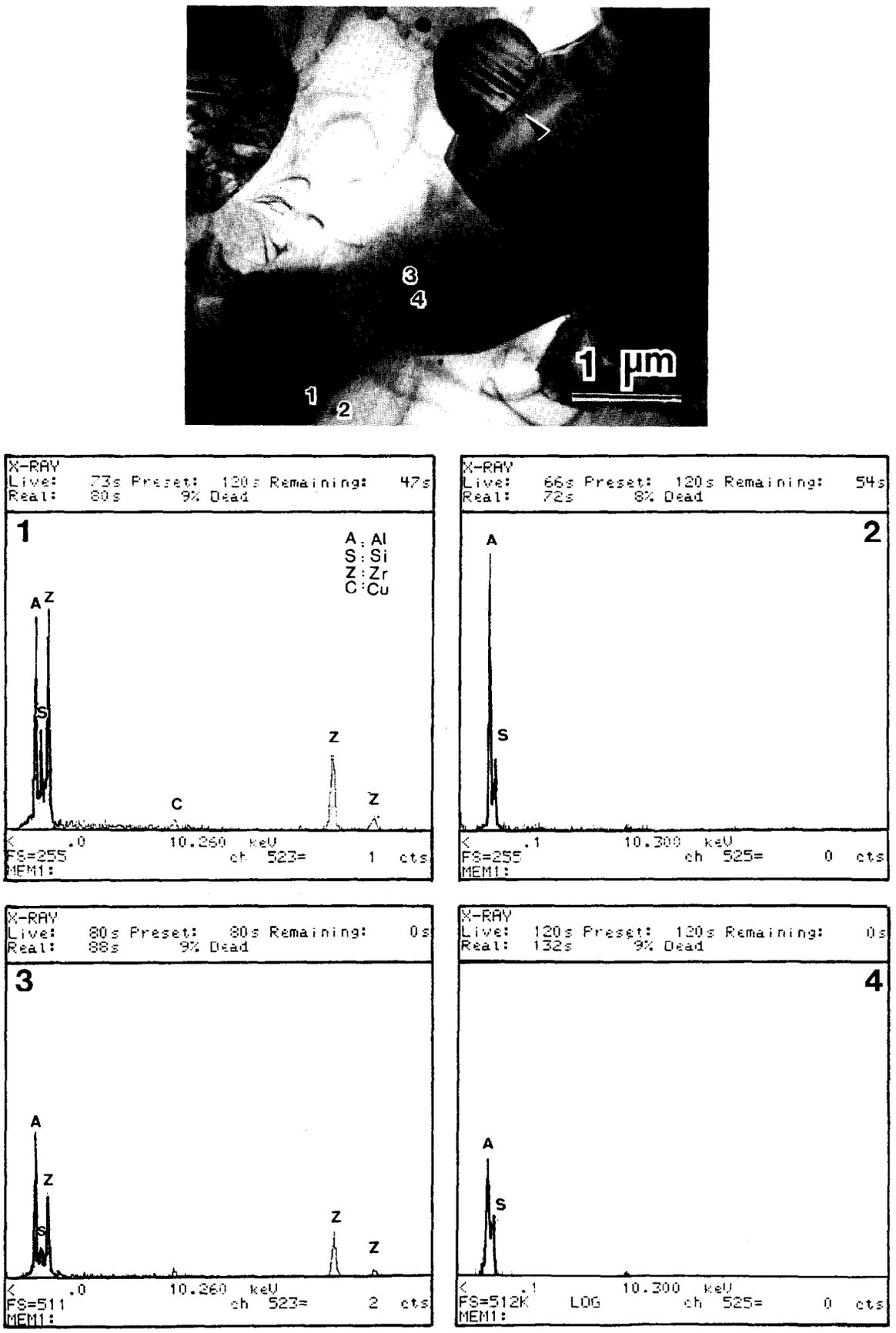

Fig. 12. TEM BF micrograph and EDX results of the intergranular and intragranular zirconia grains (1 and 3) and their mullite neighbourhood (2 and 4). The DZ-ZMC was sintered at 1700°C for 30 min.

precursors or solid powder mixtures were investigated in this study. Quantitative analysis on the micro-structural evolution of ZrO_2 and mullite matrix grains was conducted, and correlated with the processing temperature and the content of ZrO_2.

The solid solution of ZrO_2 in the mullite matrix was undetected and ZrO_2 particle-free zones were not observed in the GD- and DZ-ZMC samples, including the one with the longest heat treatment (1600°C for 24 h). This implies that the growth of ZrO_2 grains in mullite matrix cannot proceed via the process of Ostwald ripening. Grain clustering of intergranular ZrO_2 was observed, suggesting the coalescence of the ZrO_2 can occur at temperatures above 1300°C. Coarsening of intergranular and intragranular ZrO_2 particles in the mullite matrix is triggered by the mullite grain growth. The dragging of mullite grain boundaries by ZrO_2 is apparent for samples sintered at temperatures of 1400°C and above. The relationship between the grain growth of mullite and the volume fraction and size of ZrO_2 inclusions can be verified, but not well described by Zener's equation.

The advantages of the gel–process over reaction-sintering to prepare ZMCs with fine microstructure are clearly revealed in this work. A lower sintering temperature offers a higher densification rate and smaller grain size, thereby resulting in more *t*-phase zirconia and smaller grain size of mullite.

Acknowledgement

This work was supported by National Science Council in Taiwan under contract numbers NSC 81-0405-E002-25 and 82-0405-E002-245.

References

1. Claussen, N. & Ruhle, M., Design of transformation-toughened ceramics. In *Science and Technology of Zirconia III*, Advances in Ceramics, Vol. 24, eds S. Somiya, N. Yamamoto & H. Yanagida, The American Ceramics Society, Westerville, OH, 1988, p. 137.
2. Lange, F. F., Low thermal conductivity silicon nitride/zirconia composite ceramics. US Patent 4 640 902, 3 Feb. 1987.
3. Rincon, J. M. & Moya, J. S., Microstructural study of toughened ZrO_2/mullite ceramic composition obtained by reaction sintering with TiO_2. *Br. Ceram. Trans. J.*, **85** (1986) 201–6.
4. Garvie, R. C., Improved thermal shock resistant refractories from plasma-dissociated zircon. *J. Mater. Sci.*, **14** (1979) 817–22.
5. Kibbel, B. W. & Heuer, A. H., Ripening of inter- and intragranular ZrO_2 particles ZrO_2-toughened Al_2O_3. In *Science and Technology of Zirconia II*, Advances in Ceramics, Vol. 12, The American Ceramics Society, Westerville, OH, 1984, pp. 415–24.
6. Wei, W., Ph. D. Thesis, Case Western Reserve University, July 1986.
7. Wallace, J. S., Petzow, G. & Claussen, N., Microstructure and property development of in situ-reacted mullite–ZrO_2 composites. In *Science and Technology of Zirconia II*, Advances in Ceramics, Vol. 12, The American Ceramics Society, Westerville, OH, 1984, pp. 436–42.
8. Descamps, P., Sakaguchi, S., Poorteman, M. & Cambier, F., High-temperature characterization of reaction-sintered mullite–zirconia composites. *J. Am. Ceram. Soc.*, **74**(10) (1991) 2476–81.
9. Prochazka, S., Wallace, J. S. & Claussen, N., Microstructure of sintered mullite–zirconia composites. *J. Am. Ceram. Soc.*, **66** (1983) C125–7.
10. Miranzo, P., Pena, P., de Aza, S., Moya, J. S., Ma Rinco, J. & Thomas, G., TEM study of reaction-sintered zirconia–mullite composites with CaO and MgO additions. *J. Mater. Sci.*, **22** (1987) 2987–92.
11. Leriche, A., Mechanical properties and microstructures of mullite–zirconia composites. In *Mullite and Mullite Matrix Composites*. Ceramic Transactions, Vol. 6, eds S. Somiya, R. F. Davis & J. A. Pask, The American Ceramics Society, Westerville, OH, 1990, pp. 541–52.
12. Pena, P., Miranzo, P., Moya, J. S. & de Aza, S., Multicomponent toughened ceramic materials obtained by reaction sintering, Part I–System ZrO_2–Al_2O_3–SiO_2–CaO. *J. Mater. Sci.*, **20** (1985) 2011–22.
13. Dinger, T. R., Krishnan, K. M., Thomas, G., Osendi, M. I. & Moya, J. S., Investigation of ZrO_2/mullite solid solution by energy dispersive X-ray spectroscopy and electron diffraction. *Acta. Metall.*, **32**(10) (1984) 1601–7.
14. Schneider, H., Transition metal distribution in mullite. In *Mullite and Mullite Matrix Composites*, Ceramic Transactions, Vol. 6, eds S. Somiya, R. F. Davis & J. A. Pask, The American Ceramics Society, Westerville, OH, 1990, pp. 135–58.
15. Ho, Y. F. & Wei, W. J., Reaction sintering of zirconia–mullite composites. In *Proc. 1992 Annual Conf. Chinese Soc. for Mater. Sci.*, 24–26 April 1992, pp. 470–1.
16. Low, I. M. & McPersonal, R., Crystallization of gel-derived mullite–zirconia composites. *J. Mater. Sci.*, **24** (1989) 951–8.
17. Shiga, H., Katayama, K., Tsunatori, H. & Ismail, G. M. U., Sol gel synthesis and sintering of oxide-doped mullite–ZrO_2 composite powders. *Ceram. Powder Sci. IV*, (1990) 457–62.
18. Holmstrom, M., Chartier, T. & Boch, P., Reaction-sintered ZrO_2–mullite composites. *Mater. Sci. Eng.*, **A109** (1989) 105–9.
19. Mader, W., On the electron diffraction contrast caused by large inclusions. *Phil. Mag. A*, **55**(1) (1987) 59–83.
20. Lange, F. F. & Hirlinger, M. M., Hindrance of grain growth in Al_2O_3 by ZrO_2 inclusion. *J. Am. Ceram. Soc.*, **67**(3) (1984) 164–8.
21. Reed-Hill, R. E., *Physical Metallurgy Principles*, Van Nostrand, Princeton, NJ, 1973, p. 138.
22. Wei, W. & Halloran, J. W., Transformation kinetics of diphasic aluminosilicate gels. *J. Am. Ceram. Soc.*, **71**(7) (1988) 581–7.
23. Moya, J. S., Private communication, September 1994.